

# Drastic annealing effects in transport properties of single crystals of the $\text{YbNi}_2\text{B}_2\text{C}$ heavy fermion system

M. A. Avila,\* S. L. Bud'ko, and P. C. Canfield  
*Ames Laboratory and Department of Physics and Astronomy  
Iowa State University, Ames, IA 50011  
(Dated: February 1, 2008)*

We report temperature dependent resistivity, specific heat, magnetic susceptibility and thermoelectric power measurements made on the heavy fermion system  $\text{YbNi}_2\text{B}_2\text{C}$ , for both as grown and annealed single crystals. Our results demonstrate a significant variation in the temperature dependent electrical resistivity and thermoelectric power between as grown crystals and crystals that have undergone optimal (150 hour,  $950^\circ\text{C}$ ) annealing, whereas the thermodynamic properties: ( $c_p(T)$  and  $\chi(T)$ ) remain almost unchanged. We interpret these results in terms of redistributions of local Kondo temperatures associated with ligandal disorder for a small ( $\sim 1\%$ ) fraction of the Yb sites.

PACS numbers: 74.70.Dd, 75.30.Mb, 72.15.Qm

Among the rich variety of physical phenomena displayed by the  $\text{RNi}_2\text{B}_2\text{C}$  nickel boro-carbide family<sup>1,2,3,4</sup>,  $\text{YbNi}_2\text{B}_2\text{C}$  (Yb-1221) is unique so far in its behavior as a heavy fermion system<sup>5,6</sup> with an electronic specific heat coefficient,  $\gamma \approx 500\text{mJ/molK}^2$ , and a Kondo temperature,  $T_K \approx 10\text{K}$ : a temperature scale that is conveniently isolated from other characteristic temperatures such as superconducting or magnetic condensates ( $T_c, T_N < 0.03\text{K}$ , if they exist at all), and crystal electric field splitting ( $T_{cef} \approx 100\text{K}$ )<sup>7,8</sup>. The heavy fermion behavior is understood as a consequence of the fact that the ytterbium  $4f$  levels easily hybridize with the electronic conduction band levels near the Fermi surface. Such heavy electron systems often display many unusual physical properties<sup>9</sup>, one common example being disorder-related variation in the behavior of different samples of the same compound<sup>9,10</sup>.

Recently the effects of annealing on the electrical resistivity of R-1221 single crystals ( $\text{R} = \text{Y, Gd-Lu}$ ) were studied<sup>11</sup>, and once again Yb-1221 showed anomalous properties in comparison to other members of the series. Whereas annealing of crystals with  $\text{R} = \text{Y, Lu, Tm-Gd}$  simply leads only to changes in the residual resistivity, radical changes in  $R(T)$  behavior were observed for Yb-1221 over the full ( $2\text{K} - 300\text{K}$ ) temperature range. The change in  $R(T)$  was so dramatic that comparison of normalized resistance curves  $R(T)/R(300)$  became highly questionable.

To overcome this problem and better understand what is happening to the Yb-1221 crystals as they go through annealing processes, in the present work careful resistivity measurements were made on Yb-1221 crystals cut into well-defined geometries, such that no normalization is necessary and direct comparison of  $\rho(T)$  for different samples and annealing procedures is possible. The results, in combination with measurements of specific heat, magnetic susceptibility and thermoelectric power, allow us to propose a mechanism in which optimal annealing is essentially affecting the ligandal disorder associated with a small fraction ( $\sim 1\%$ ) of the Yb sites. But given that

Yb is a hybridizing rare earth ion, it is far more sensitive to such disorder than its non-hybridizing neighbors. Yb-1221 then presents a model heavy fermion system that allows for the study of how small changes in disorder can lead to dramatic changes in transport properties.

Single crystals of  $\text{YbNi}_2\text{B}_2\text{C}$  were grown from  $\text{Ni}_2\text{B}$  flux at high temperatures as described elsewhere<sup>4,5</sup>. Single crystal plates ( $4 \times 4 \times 0.5\text{mm}^3$  typical dimensions) were selected, polished and cut into bars (typically  $1 - 2\text{mm}$  in length and  $0.1\text{mm}^2$  cross section) with the length along the  $[100]$  direction using a wire saw. Once cut the samples were cleaned with toluene and methanol, placed in a Ta foil envelope and then placed into the quartz insert of a high vacuum-annealing furnace. The insert was continuously pumped down to a pressure of less than  $10^{-6}\text{Torr}$  during the annealing schedule which consisted of a one hour dwell at  $200^\circ\text{C}$  to outgas, followed by the chosen number of hours anneal at  $950^\circ\text{C}$ , followed by a 3-4 hour cool down to room temperature. Once the schedule was completed, the insert was brought to atmospheric pressure and the samples removed. Each sample was annealed only once, and for the magnetization and specific heat data the same sample was used to collect the un-annealed and annealed data sets.

Electrical resistance measurements were performed on Quantum Design MPMS systems operated in external device control (EDC) mode, in conjunction with Linear Research LR400/LR700 four-probe ac resistance bridges, allowing measurements down to  $1.8\text{K}$ . The electrical contacts were placed on the samples in standard 4-probe linear geometry, using Pt wires attached to a sample surface with Epotek H20E silver epoxy. For each slab, the sample weight and dimensions were carefully measured and an evaluation of the sample densities ( $8.3 \pm 0.3\text{g/cm}^3$ ) was used to estimate an upper limit of  $\pm 15\%$  for the overall geometry-related errors in calculating resistivity  $\rho = RA/l$ . Susceptibility measurements were made on these same MPMS systems, using their standard DC magnetization operating modes, and for the sample oriented in both  $H||c$  and  $H||a$  directions. Specific heat

measurements were made on a Quantum Design PPMS system containing both specific heat and  $^3\text{He}$  options, allowing measurements down to  $0.35\text{K}$ .

Thermoelectric power measurements were made on a commercial MMR Technologies Seebeck System, which uses a compressed  $\text{N}_2$  gas based Joule-Thompson refrigerator allowing temperature control down to  $90\text{K}$ . The sample Seebeck coefficient  $S(T)$  is obtained by comparison with a reference constantan wire.

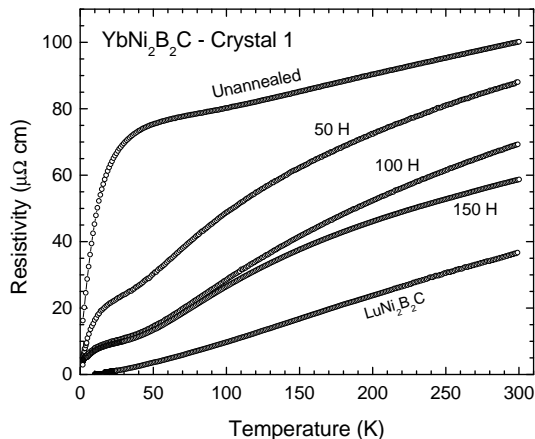


FIG. 1: Temperature dependence of the electrical resistivity of several pieces of Yb-1221 cut from crystal 1, for different annealing times at  $950^\circ\text{C}$ . A measurement on unannealed Lu-1221 is also included for comparison.

The temperature dependence of the electrical resistivity for four bars cut from a single crystal (crystal 1) is shown in fig. 1. There is a substantial change in the temperature dependence as well as a reduction in the magnitude of the resistivity as the annealing time is increased. For increasing annealing times the resistivity of Yb-1221 approaches that of  $\text{LuNi}_2\text{B}_2\text{C}$  (shown as the lowest resistivity curve in fig. 1)<sup>12</sup>.

Figure 2 presents a similar set of annealing data from a second crystal (crystal 2). In this case several shorter time anneals were performed in addition to the 50 hour and 150 hour anneals. Whereas the longer annealing times lead to qualitatively similar resistivity curves to those shown in fig. 1, the shorter annealing times manifest a different behavior: an increase in the higher temperature resistivity followed by a decrease in the lower temperature resistivity. Qualitatively similar behaviors were found for several other crystals. For low temperatures, resistivity is monotonically reduced with increasing annealing time, whereas for temperature nearer to room temperature there can be an initial rise in resistivity followed by an ultimate decrease in resistivity for increasing annealing times. Ultimately, for annealing times on the order of 150 hours, the resistivity is increasingly approaching that of  $\text{LuNi}_2\text{B}_2\text{C}$ .

The temperature dependent resistivity for 150 hour an-

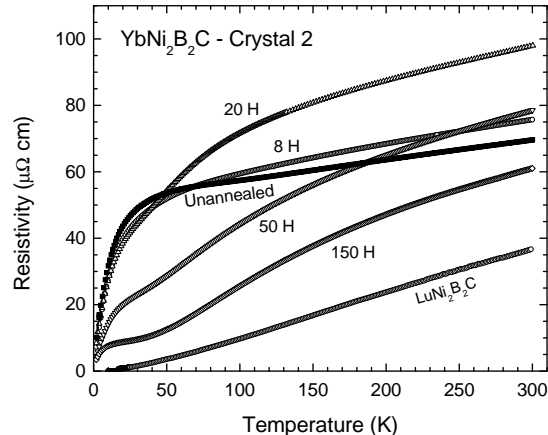


FIG. 2: Temperature dependence of the electrical resistivity of several pieces of Yb-1221 cut from crystal 2. Note that for shorter annealing times the higher temperature resistivity increases. For longer annealing times the resistivity data is quantitatively similar to the data shown in figure 1.

neals (figs. 1 and 2) are consistent with a Yb-based intermetallic that has  $T_K \approx 10\text{K}$ . There is an initial decrease in resistivity with decreasing temperature. The broad shoulder near  $200\text{K}$  is very likely associated with the thermal depopulation of the upper CEF levels. There is a beginning of a resistance minimum near  $30\text{K}$ , followed by a sharp decrease in resistivity associated with coherence as the sample is cooled through  $T_K$ . These data are almost precisely what would be expected from a text book example of a low  $T_K$  intermetallic.

In contrast with the results of resistivity measurements, 150 hour annealing at  $950^\circ\text{C}$  causes only minor changes (if any) in the material's bulk thermodynamic properties. In fig. 3 we show measurements of the temperature dependence of (a) specific heat and (b) inverse magnetic susceptibility performed on two pieces cut from crystals 3 and 4 respectively, before and after they were annealed for  $150\text{h}@950^\circ\text{C}$ . The general features of these curves are consistent with previously reported measurements on unannealed Yb-1221 crystals<sup>5</sup>. The fact that the bulk thermodynamic properties do not change, within experimental limits, gives support to the hypothesis that annealing is affecting only a very small fraction of the sample, and also helps to rule out any possibility of major structural changes such as phase separation, decomposition, corrosion, oxidation or other such degradations to the crystalline lattice.

Based on the data presented in figures 1-3 as well as previous work on the non-hybridizing members or the  $\text{RNi}_2\text{B}_2\text{C}$  series (e.g.  $\text{R} = \text{Y}, \text{Lu}, \text{Tm-Gd}$ )<sup>11</sup> it appears that annealing single crystals of  $\text{RNi}_2\text{B}_2\text{C}$  can cause significant changes in the electrical resistivity. For the samples of  $\text{LuNi}_2\text{B}_2\text{C}$  or  $\text{YNi}_2\text{B}_2\text{C}$  (as well as the local moment members) this increased perfection simply leads to

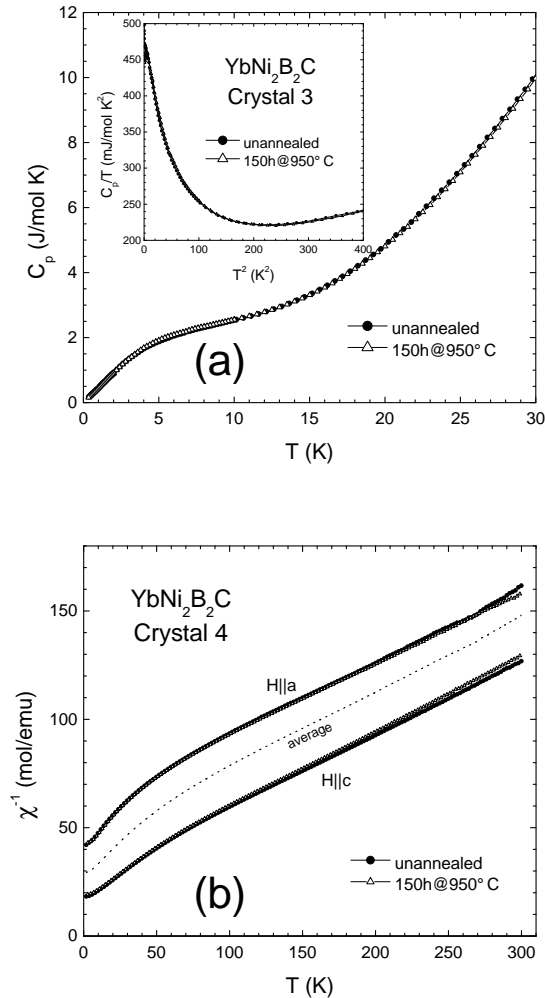


FIG. 3: (a) Specific heat of Yb-1221 crystal 3, before and after annealing at  $950^\circ\text{C}$  for 150 hours. The inset shows the  $T^2$  dependence of the linear term  $c_p/T$  at the lowest temperatures. (b) Inverse susceptibility of Yb-1221 crystal 4 for both orientations  $H||c$  and  $H||a$ , before and after annealing at  $950^\circ\text{C}$  for 150 hours. Annealing does not significantly change the crystal's thermodynamic properties.

a reduction of the residual resistivity. On the other hand for the case of YbNi<sub>2</sub>B<sub>2</sub>C, disorder around the hybridizing Yb ion can very easily lead to a change of the local Kondo temperature. This observation leads to a simple hypothesis: a small number of Yb sites have a distribution of Kondo temperatures that can have values ranging from 10 K or lower up to above room temperature. This distribution in  $T_K$  values is associated with a distribution of Yb-ligandal environments. With annealing, this disorder is reduced and a diminishingly small number of Yb sites have Kondo temperatures different from  $T_K \approx 10\text{K}$ .

The first question that can be simply addressed is:

what percentage of Yb sites would need to have Kondo temperatures above room temperature to account for the  $\sim 40\mu\Omega\text{cm}$  excess resistivity found near room temperature in the unannealed samples? This can be estimated by using the expression for the increase in resistivity associated with a Kondo impurity for temperatures below the Kondo temperature associated with the impurity<sup>13</sup>:

$$\Delta\rho_{max} = \frac{\hbar}{e^2} \frac{4\pi c}{pk_F} (2l+1) \quad (1)$$

where  $c$  is the concentration of Yb “impurities”,  $k_F$  is the Fermi momentum,  $p$  is the number of electrons per atom, and  $l$  is the ytterbium  $4f$  angular momentum. Using  $l = 3$ ,  $p = 3$  and  $k_F \approx 3.7 \times 10^7 \text{cm}^{-1}$  [refs. 14,15] in this equation, we estimate  $\Delta\rho_{max} = 30\mu\Omega\text{cm}$  for every 1% concentration of disordered Yb sites with  $T_K$  greater than room temperature. This means that only a few percent of the Yb ions need to have Kondo temperatures different from the expected value of  $T_K \approx 10\text{K}$ , to produce a significant increase in resistivity that is seen in figs. 1 and 2. It should be noted that the above calculation is at best semi-quantitative (i.e. should be trusted to only within factors of two), but it does demonstrate that our working hypothesis is a viable one.

The evolution of the temperature dependent resistivity can be understood then by simply invoking a reduction of ligandal disorder with annealing. For long time anneals the number of Yb ions that have  $T_K$  values higher than 10K has been reduced to a negligible amount. This leads to the nearly classical  $\rho(T)$  curves seen in figs. 1 and 2. For smaller annealing times the higher temperature resistivity of the sample can either increase or decrease, depending upon the nature (quantity and type) of disorder in the as-grown sample. As the ligandal disorder is annealed away there is no reason to assume that intermediate states (of crystallographic order) will have  $T_K$  values that monotonically approach 10K: e.g. as seen in crystal 2 (fig. 2) small annealing times appear to be populating configurations with higher  $T_K$  values. We have performed annealing studies on five different groups of samples cut from crystals from different batches. In every case the long time anneals ( $\sim 150$  hours) approach the resistivity data shown in figs. 1 and 2. The behavior illustrated by figs. 1 and 2 appears to be a generic behavior for Yb-1221 samples prepared in this manner.

If indeed the changes in  $\rho(T)$  are due to changes in ligandal disorder in a small fraction of the Yb-sites, then we would anticipate that any bulk, thermodynamic property of the material should not be significantly affected by the annealing process. For  $c_p(T)$ , the change in the number of  $T_K \approx 10\text{K}$  Yb sites (on the order of 98% to 100%) that occurs with annealing is so small that it is not resolvable in our measurements (fig. 3a) on the same piece of sample (as grown and annealed). The measured curves are essentially indistinguishable for  $0.35\text{K} \leq T \leq 30\text{K}$ . For  $\chi(T)$ , annealing effects are equally indistinguishable. The vast majority of the Yb sites are acting as Yb<sup>+3</sup> at

high temperatures and, again, a change of a percent or two is not distinguishable in our measurements.

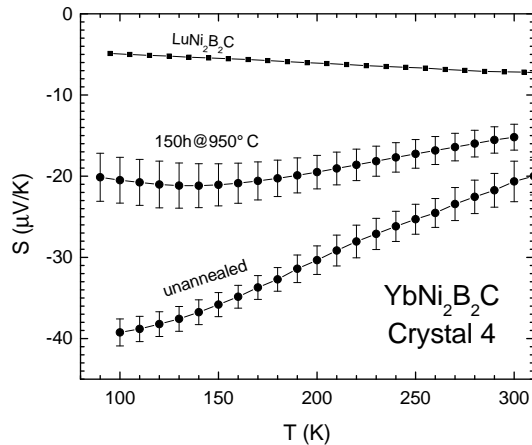


FIG. 4: Absolute thermopower of several samples of Yb-1221 cut from crystal 4 (the unannealed data manifold is the average of data from three samples, and the annealed data manifold is the average of data from two samples that were annealed at  $950^{\circ}\text{C}$  for 150 hours). A measurement on unannealed Lu-1221 is also included for comparison.

Finally, since the assumed disorder affects the DOS profile near the Fermi surface, one should expect significant changes in the material's thermoelectric power. Figure 4 shows the temperature dependence of the Seebeck coefficient  $S(T)$  obtained by measuring several pieces cut out of Yb-1221 crystal 4. Three pieces were measured after cutting, and two other pieces were measured after annealing for  $150\text{h}@950^{\circ}\text{C}$ , and the results for these two groups of data were averaged. An unannealed Lu-1221 sample was also measured for comparison. Both the unannealed Yb-1221 and Lu-1221 data agree very well with previously reported measurements on these compounds<sup>16</sup>, although there is a sample-to-sample scatter (as indicated by the error bars) in  $S(T)$  in our data.

The limited temperature range of our experimental equipment does not allow us to clearly observe the most prominent feature in such measurements, which is a large negative peak in  $S(T)$  just below  $100\text{K}$ <sup>16</sup> but the high-temperature data of our samples is seen to follow the generally expected behavior within the framework of the

Coqblin-Schrieffer model<sup>17,18,19</sup>, and the disorder-related effects discussed here. For the unannealed samples, the response should be a combination of a low  $T_K$  Kondo lattice and single-Yb “impurity” effects with high  $T_K$  values, both of which are known to greatly increase the absolute values of  $S(T)$  for  $T \gg T_K$ . Annealing will then have the effect of reducing the impurity contribution, which in our case results in a reduction of roughly 50% (from  $\sim 40$  to  $\sim 20\mu\text{V/K}$ ) in the magnitude of the thermopower response near the peak, whose position also seems to shift to slightly higher temperatures. The resulting curves for annealed Yb-1221 samples move towards the Lu-1221 reference, but still maintain the enhanced contribution coming mostly from the Kondo Lattice with CEF splitting<sup>18</sup>.

In conclusion, we have shown how annealing of single crystal YbNi<sub>2</sub>B<sub>2</sub>C leads to dramatic changes in its transport behavior. These changes can be understood as a consequence of the effects of ligandal disorder that leads to locally large values of  $T_K$  associated with a small fraction of local Yb sites. This small number of high  $T_K$  sites leads to large enhancements in electrical resistivity and thermoelectric power that are very sensitive to the amount of time the crystal is annealed. Increased annealing times reduce the number of perturbed Yb sites and lead to more classical, and simply understood, temperature dependencies of the transport properties. To this extent, YbNi<sub>2</sub>B<sub>2</sub>C continues to be a model heavy fermion compound: not only from the fact that other characteristic energy scales are well separated from  $T_K$  in this material<sup>5</sup>, but also because it allows for more detailed investigations of exactly how different disturbances in the vicinity of Yb sites affect the hybridization of its  $4f$  level with conduction states and the hybridized Kondo lattice. This is a near ubiquitous problem in heavy fermion systems and will hopefully be addressed more fully by future diffraction measurements aimed at determining the exact nature of the hypothesized ligandal disorder.

### Acknowledgments

We are thankful to F. Steglich for suggesting the experiments on thermoelectric power. Ames Laboratory is operated for the US Department of Energy by Iowa State University under Contract No. W-7405-Eng-82. This work was supported by the Director for Energy Research, Office of Basic Energy Sciences.

\* Electronic address: avila@ameslab.gov

<sup>1</sup> R. Nagarajan, C. Mazumdar, Z. Hossain, S. K. Dhar, K. V. Gopalakrishnan, L. C. Gupta, C. Godart, B. D. Padalia, and R. Vijayaraghavan, Phys. Rev. Lett. **72**, 274 (1994).

<sup>2</sup> R. J. Cava, H. Takagi, B. Batlogg, H. W. Zandbergen, J. J. Krajewski, W. F. P. Jr., R. B. van Dover, R. J. Felder, T. Siegrist, K. Mizuhashi, et al., Nature **367**, 252 (1994).

<sup>3</sup> P. C. Canfield, S. L. Bud'ko, B. K. Cho, W. P. Beyermann,

and A. Yatskar, J. Alloys Compds **250**, 596 (1997).

<sup>4</sup> P. C. Canfield, P. L. Gammel, and D. J. Bishop, Physics Today **51**, 40 (1998).

<sup>5</sup> A. Yatskar, N. K. Budraa, W. P. Beyermann, P. C. Canfield, and S. L. Bud'ko, Phys. Rev. B **54**, R3772 (1996).

<sup>6</sup> S. K. Dhar, R. Nagarajan, Z. Hossain, E. Tominez, C. Godart, L. C. Gupta, and R. Vijayaraghavan, Solid State Commun. **98**, 985 (1996).

- <sup>7</sup> U. Grasser, P. Allenspach, F. Fauth, W. Henggeler, J. Mesot, A. Furrer, S. Rosenkranz, P. Vorderwisch, and M. Buchgeister, *Z. Phys. B* **101**, 345 (1996).
- <sup>8</sup> M. Rams, K. Krolas, P. Bonville, J. A. Hodges, Z. Hossain, R. Nagarajan, S. K. Dhar, L. C. Gupta, E. Alleno, and C. Godart, *J. Magn. Magn. Mater.* **219**, 15 (2000).
- <sup>9</sup> G. R. Stewart, *Rev. Mod. Phys.* **56**, 755 (1984) and references therein.
- <sup>10</sup> W. Franz, A. Griessel, F. Steglich, and D. Wohlleben, *Z. Phys. B* **31**, 7 (1978).
- <sup>11</sup> X. Y. Miao, S. L. Bud'ko, and P. C. Canfield, *J. Alloys Compnds.* **338**, 13 (2002).
- <sup>12</sup> K. O. Cheon, I. R. Fisher, V. G. Kogan, P. C. Canfield, P. Miranovic, and P. L. Gammel, *Phys. Rev. B* **58**, 6463 (1998).
- <sup>13</sup> J. D. Thompson and Z. Fisk, *Phys. Rev. B* **31**, 389 (1985).
- <sup>14</sup> V. G. Kogan, M. Bullock, B. Harmon, P. Miranovic, L. Dobrosavljevic-Grujic, P. L. Gammel, and D. J. Bishop, *Phys. Rev. B* **55**, 8693 (1997).
- <sup>15</sup> S. B. Dugdale, M. A. Alam, I. Wilkinson, R. J. Hughes, I. R. Fisher, P. C. Canfield, T. Jarlborg, and G. Santi, *Phys. Rev. Lett.* **83**, 4824 (1999).
- <sup>16</sup> K. D. D. Rathnayaka, D. G. Naugle, S. Lim, M. C. de Andrade, R. P. Dickey, A. Amann, M. B. Maple, S. L. Bud'ko, P. C. Canfield, and W. P. Beyermann, *Int. J. Mod. Phys.* **13**, 3725 (1997).
- <sup>17</sup> V. Zlatic, I. Milat, B. Coqblin, and G. Czycoll, *cond-mat/0110179* (2001).
- <sup>18</sup> A. K. Bhattacharjee and B. Coqblin, *Phys. Rev. B* **13**, 3441 (1976).
- <sup>19</sup> B. Coqblin and J. R. Schrieffer, *Phys. Rev.* **185**, 847 (1969).